Preprints, 10th IFAC International Symposium on
Advances in Automotive Control
Columbus, Ohio, USA, August 28-30, 2022

Jerk Minimization for a Novel Engine Crank Mechanism using LQG Control

Neeraj Shidore*, Madhusudan Raghavan*

**General Motors Research and Development, Warren, USA*
(Tel: 586-985-9487; e-mail: neeraj.shidore@gm.com).

Abstract: The paper presents the development of LQG (Linear Quadratic Gaussian) Control to minimize the jerk , during the actuation of a novel engine crank mechanism ,for a hybrid electric vehicle. The operation of the novel mechanism is explained in detailed. Open loop simulation results show an undesirable jerk , which is perceptible to the driver, during the actuation of this mechanism. A closed loop LQG controller is then formulated to minimize the jerk and provide a smooth engine start. The formulation of the plant model, observer design is explained. Incremental control is used to approximate jerk from the output equation. Finally, closed loop simulation results show a smooth engine crank while minimizing the undesirable jerk.

Keywords: Planetary Starter, LQG control, tip in response, P2 hybrid .

1. INTRODUCTION

A hybrid architecture, where-in the electric motor generator unit (MGU) is connected to the driveline in between the engine and the transmission (Figure 1) is referred to as a 'P2'.

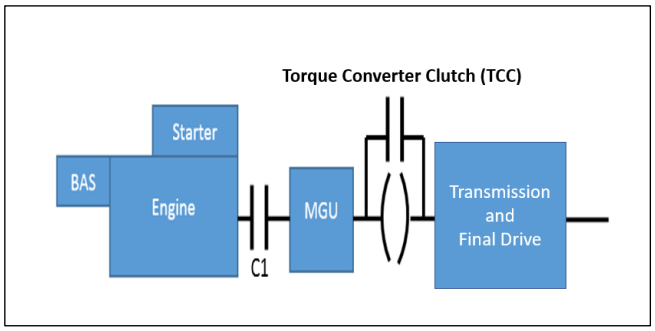

Figure 1. P2 hybrid vehicle architecture.

A significant challenge for the P2 hybrid architecture , is the need for quick reconnection of the disconnected engine to the drivetrain , during a 'tip-in' or change of mind event. A tip in or change of mind event occurs during vehicle braking or coasting (engine is off and disconnected) and is initiated by a sudden acceleration demand by the driver. In such a scenario, the engine must be cranked and connected to the driveline in the shortest possible time, to fulfill the driver acceleration demand. This is even more important when the motor power is a small fraction of the engine power and cannot support the acceleration power requirements on its own. The tip in maneuver is therefore a critical drive quality metric for a P2 [1], [2]. This tip-in related drive quality metric has two components to it: the time to acceleration (from the initial accelerator pedal command), and the quality of the acceleration, which includes the disturbance during the engine cranking event [3].

As shown in figure 1, two starting mechanisms are traditionally used to crank the engine, either a pinion starter [4], or the BAS (Belt Alternator Starter) Machine [5]. Each of these two devices offer a trade-off between several factors: the tip-in drivability metric, fuel economy benefits, cost, packaging, ease of control, robustness, and cold weather performance. The authors have proposed a novel mechanism to crank a P2 hybrid powertrain, as an alternative to the above two mechanisms, called the planetary starter [6]. By eliminating the need for a starter or a BAS machine, this mechanism eliminates the need to carry two electrical machines onboard (the P2 MGU being the primary machine). This paper discusses a controls approach to improve the tip-in metric with the planetary starter by elimination of the jerk during engine crank. Other aspects like packaging, cost, which are equally important when making the final choice of the start mechanism, are beyond the scope of the paper.

1.1 Literature review

Wu et al discuss the different powertrain architectures in [1] . The tradeoff between drivability and fuel economy for a mild hybrid P2 drivetrain is discussed in [2]. Juach et al [3] discuss a model for drivability and control for a hybrid vehicle. Hao et al [4] discuss a high-performance starter as an alternative option to the concept proposed in this paper. Some details on the planetary starter can be found in the patent by Raghavan and Shidore [6].

1.2 Paper overview

The flow of the paper is as follows: Section 2 gives an overview of the planetary starter architecture, which is the novel mechanism for engine cranking that will be controlled by the LQG control. This section also provides detail on the vehicle drive scenario (change of mind engine crank) and the vehicle propulsion system model that will be used to access the effectiveness of the LQG Control. Open loop results show the need of closed loop control, during the actuation of the

novel crank mechanism. Section 3 lays out the development of the control algorithm in detail. Section 4 shows simulation results that compare the results of engine crank with and without the LQG controller. Section 5 is the conclusion.

2. PLANETARY STARTER

2.1 Architecture

Figure 2 shows the architecture of the planetary starter. A simple planetary gear is used along with a clutch and brake (or clutch) to realize the planetary starter.

The engine is connected to the carrier node, while the P2 MGU is connected to the sun gear. The other end of the P2 MGU shaft is connected to the torque converter pump. The Ring Gear is free-wheeling but can be forced to be at zero speed by using brake (B), which is between the ring gear and a non - moving element like the transmission housing. The clutch (C), when closed, forces the ring gear and the carrier to turn at the same speed, thus forcing the planetary gear ratios to reduce to unity. Schematically, the clutch C can be between any two elements of the planetary. Table 1 shows the different modes possible with the clutch (C) and the brake (B) being in the closed or open position.

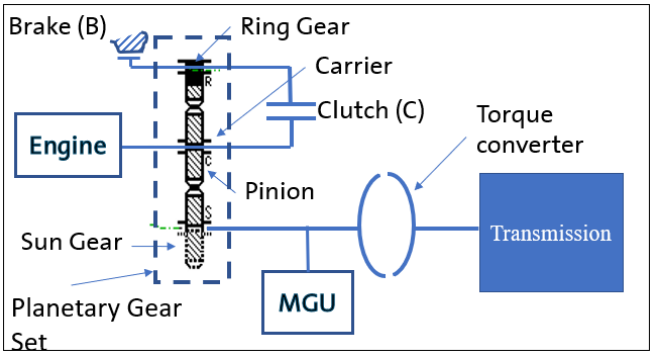

Figure 2. Planetary Starter Architecture

Table 1. Planetary States of Operation

Vehicle State	Brake (B)	Clutch (C)
EV Driving	Open	Open
Engine Crank	Closed	Open
Hybrid Driving	Open	Closed

During EV driving, both brake B and clutch C are open , effectively disengaging the engine from the drive train. The engine crank and the hybrid driving vehicle states are explained in detail below. Figure 3 shows the operation of the planetary starter during an engine crank event. At 43 seconds, the vehicle is in EV mode , and the P2 motor is at around 1650 RPM (blue). This is also the speed of the sun gear. The ring gear is 'free-wheeling' and based on the planetary gear ratio, is spinning at 500 RPM. The carrier (engine) speed is zero since the engine is disconnected from the drivetrain and is assumed to be at zero speed. All speeds are shown on the primary Y axis. At about 43.03 seconds, there is a need to crank the engine, due to a sudden tip in by the driver. As a result, brake B is engaged (pink and pink Y axis). This causes the carrier (engine speed) to increase from zero. As soon as the engine speed has reached firing speed , the brake is dis-engaged, and the engine is able to increase its own speed using spark and fuel (around 43.4 seconds). There is a need to bring the engine up to firing speed before throttle and spark are actuated, and therefore , the brake actuation precedes throttle.

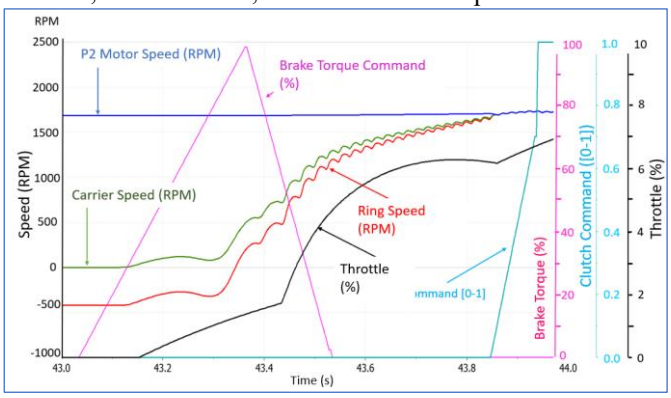

Figure 3. Engine crank actuation with planetary starter

The engine speed is then controlled to match the P2 MGU speed (around 43.8 seconds). When the carrier (engine) and the sun (P2 MGU) speeds are close, the clutch C is closed (cyan, command 0 to 1), which causes all elements of the planetary to spin at the same speed, i.e. the engine and the P2 motor are now at the same speed, as should be the case in a P2 where there is no gear ratio between the engine and the P2 motor. Once clutch C is closed, engine can provide traction torque to support the acceleration demand.

2.2 P2 vehicle model for planetary drive quality evaluation

To emulate the plant, the entire driveline was modelled in AMESIM.To be able to view the details of the powertrain model, the figure representing the powertrain model is presented as a full page in Appendix A at the end of the paper. This model also acts as the plant for the LQG [7] controller described in the next section. The planetary gear is shown in blue. All significant elements of the drivetrain have been modeled in red. Table 2 lists the parameter variable names, and description. Nominal values for a class 2B truck have been chosen for the simulation but are not stated in the paper, for brevity. In table 2, the 'transformer' is a notation commonly used in bond graphs, to suggest the ratio of flow and effort elements on either bond of the transformer. In the current context, these are used to express the gear ratios associated with the planetary (TF1 and TF2) and 2nd gear (TF3) respectively.

2.3 Open loop simulation of the P2 drivetrain for a change of mind engine crank

A vehicle drive scenario, which would provide the máximum jerk to the driveline during an engine crank event with the planetary starter was chosen. This was with the vehicle at low speeds (around 7 to 8 meters per second) , in 2nd gear and with

the torque converter clutch closed. Figure 4 shows the vehicle acceleration (red) along with the brake torque (blue), engine throttle (black) and clutch command (cyan). The brake torque and the throttle commands are in the form of impulse inputs (very short time spans).The initial brake torque causes a sudden negative vehicle acceleration (around 39.3 seconds), which can be sensed by the driver and will negatively impact the drive quality rating. The impulse nature of the torque commands also causes a sustained undesirable oscillation on the driveline. The initial jerk and sustained oscillations have a negative impact on vehicle drive quality and need to be reduced/eliminated.

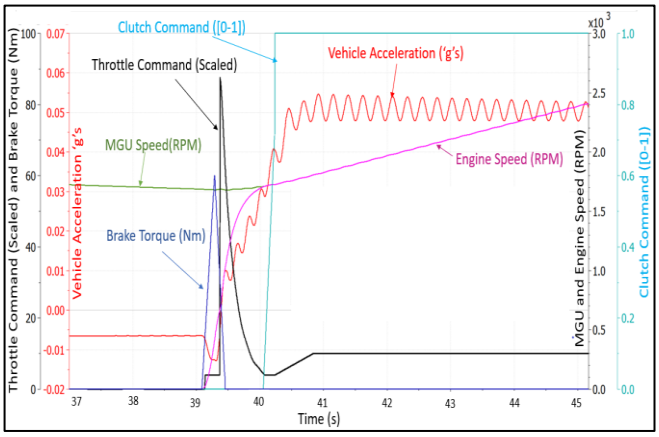

Figure 4. Actuation torques and resultant acceleration (open loop)

3. LQG CONTROL DEVELOPMENT

3.1 Plant Model Development

The dynamic equations for the plant (vehicle driveline with the planetary gear) are derived using Bond Graphs [8]. The variable names in the bond graph representation in the figure 5 below are the same as Table 2. The use of bond graphs is not a necessary step in the state space formulation.

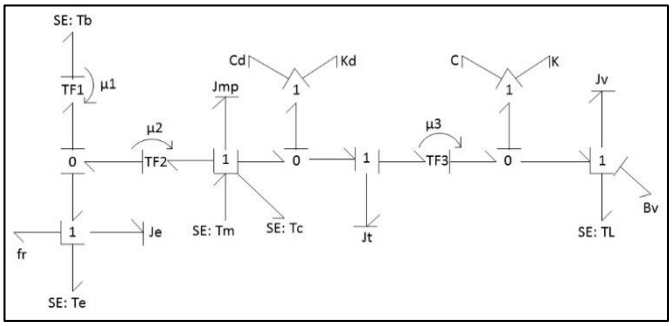

Figure 6. Bond Graph Representation of the Powertrain Model

To have integral causality for element 'Je', i.e. engine speed, the inertia of the brake element/ring gear has not been considered. Inserting an elastic element between the brake and the ring gear would enable inclusion of brake inertia but would have increased the order of the system. The inertia of the carrier and sun gears have been neglected in this exercise, but they can easily be combined with the engine and the motor inertia respectively. Integral causality for 'Je' in the bond graph is important since it allows us to use engine speed as a state. Following are the six states of the system: engine speed, motor speed, turbine speed, wheel speed, angle between motor and turbine inertias , i.e. due to the spring with stiffness Kd, angle between turbine and wheel inertias, due to spring with stiffness K. All speeds are measured, while the angles are estimated using a Kalman filter. There are two modes of operation, when clutch C is open, the plant model has 6 states (stated above). When clutch C is closed engine and motor speeds are the same, so that the system collapses to a 5th order system. The control objective is to control the motor torque to reject disturbances – throttle, brake, clutch, and vehicle load torque.

Equation (1) below shows the plant model in standard state space format .

$$\dot{X(t)} = A_O X(t) + B_O U(t) + B_{OW} W(t) \quad (1)$$

$$y(t) = C_o X(t) + v(t)$$

The subscript 'o' is for clutch C being open. $X(t)$is the state vector, $v(t)$ is the vector of sensor noise (modeled in the plant as a zero-order hold and added gaussian noise), $U(t)$ is the control input vector (motor torque) and $W(t)$ is a vector of disturbance inputs (clutch torque, throttle, brake, vehicle load).

In continuous time domain, wheel acceleration ($\dot{x_4}$) can be considered an output, which is directly linked to vehicle acceleration by a constant ratio. Using the bond graph, the state, input, and output matrices in equation (1) are as below in equations (2) through (5). When the clutch is closed, the system collapses to a 5th order. Equation (6) below is the state equation for the 5th order system. Other matrices, when clutch is closed, have not been stated in the paper for brevity.

Table 2. Vehicle drivetrain Parameters for Plant Model

Variable Name	Parameter Explanation	Unit/Formula
Ns	# Teeth on Sun Gear	
Nr	# Teeth on Ring Gear	
I_f	Final Drive Gear Ratio	
I_t	Second Gear Ratio	
K	Axle ,Prop Shaft Stiffness	Nm/deg
C	Axle ,Prop Shaft Damping	Nm/deg/s
Je	Equivalent Engine Inertia	kg m^2
rw	Wheel Radius	m
Bv	Vehicle viscous damping	0.5*rw^2 Nm/rad/s
M	Vehicle Mass	kg
rho	Air Density	kg/m^3
Mu_roll	Rolling Resistance Coeff	
Cw	Drag Coefficient	

Av	Frontal Area	m^2
Jw	Wheel Inertia	kgm^2
Jv	Equivalent Vehicle Inertia	2*Jw+M*rw^2
Kd	TCC Damper stiffness	Nm/deg
Cd	TCC Damper Damping	Nm/deg/sec
Jm	Motor Inertia	kgm^2
Jp	TC Pump Inertia	kgm^2
Jtu	TC Turbine Inertia	kgm^2
Jtr	Transmission Inertia (2nd gear, reflected to input)	kgm^2
Jpr	Prop shaft inertia reflected to trans input in 2nd gear	kgm^2
μ1	Ratio for transformer TF1 (in bond graph notation)	-Nr/(Ns+Nr)
μ2	Ratio for transformer TF2 (in bond graph notation)	(Ns+Nr)/Ns

3.2 Scaling and Discretization

Scaling has been used to formulate a numerically well-conditioned problem, given the large difference in the values of some states (speed versus angle) . MATLAB 'Prescale' command creates diagonal scaling matrices T_L and T_R. The transformation maps state vector X to W, and the state space matrices are also suitably transformed as shown in equations (7) to (10). The suffix 's' in the matrix names denotes a scaled matrix. The same operation is performed on the 5th order system. The state space systems $(A_{o,s}, B_{o,s}, C_{o,s})$ and $(A_{c,s}, B_{c,s}, C_{c,s})$, are used to design the state feedback gains (LQR).

$$A_o = \begin{bmatrix} \frac{-f}{Je} & 0 & 0 & 0 & 0 & 0 \\ 0 & \frac{-Cd}{Jmp} & \frac{Cd}{Jmp} & 0 & \frac{-Kd}{Jmp} & 0 \\ 0 & \frac{Cd}{Jt} & \frac{-Cd}{Jt} - \frac{\mu_3{}^2 C}{Jt} & \frac{\mu_3 C}{Jt} & \frac{Kd}{Jt} & \frac{-\mu_3 K}{Jt} \\ 0 & 0 & C\frac{\mu_3}{Jv} & \frac{-C}{Jv} - \frac{Bv}{Jv} & 0 & \frac{K}{Jv} \\ 0 & 1 & -1 & 0 & 0 & 0 \\ 0 & 0 & \mu_3 & -1 & 0 & 0 \end{bmatrix} \quad (2)$$

$$Bo = \begin{bmatrix} 0 & \frac{1}{Jmp} & 0 & 0 & 0 & 0 \end{bmatrix}^T \quad (3)$$

$$Bow = \begin{bmatrix} \frac{-1}{Je} & 0 & \frac{1}{\mu_1 . Je} & 0 \\ 0 & 0 & \frac{-1}{Jmp.\mu_1.\mu_2} & \frac{-1}{Jmp} \\ 0 & 0 & 0 & 0 \\ 0 & \frac{-1}{Jv} & 0 & 0 \\ 0 & 0 & 0 & 0 \\ 0 & 0 & 0 & 0 \end{bmatrix} \quad (4)$$

$$Co = [0 \quad 0 \quad \frac{C\mu_3}{Jv} \quad \frac{-C}{Jv} - \frac{Bv}{Jv} \quad 0 \quad \frac{K}{Jv}] \quad (5)$$

$$A_c = \begin{bmatrix} \frac{-f_r - Cd}{Jmpe} & \frac{Cd}{Jmpe} & 0 & \frac{-Kd}{Jmpe} & 0 \\ \frac{Cd}{Jt} & \frac{-Cd}{Jt} - \frac{\mu_3{}^2 C}{Jt} & \frac{\mu_3 C}{Jt} & \frac{Kd}{Jt} & \frac{-\mu_3 K}{Jt} \\ 0 & C\frac{\mu_3}{Jv} & \frac{-C}{Jv} - \frac{Bv}{Jv} & 0 & \frac{K}{Jv} \\ 1 & -1 & 0 & 0 & 0 \\ 0 & \mu_3 & -1 & 0 & 0 \end{bmatrix} \quad (6)$$

$$W = T_L . X \quad (7)$$

$$A_{o,s} = T_L . A_o . T_R \quad (8)$$

$$B_{o,s} = T_L . B_o \quad (9)$$

$$C_{o,s} = C_o . T_R \quad (10)$$

To design the Kalman filter gains, matrices C_{om} and C_{cm} are defined as in (11) and (12). Matrix C_{om} is the output matrix for the Kalman filter when the clutch C is open, while C_{cm} is the output matrix for the Kalman filter when the clutch is closed.

$$C_{om} = \begin{bmatrix} 1 & 0 & 0 & 0 & 0 & 0 \\ 0 & 1 & 0 & 0 & 0 & 0 \\ 0 & 0 & 0 & 1 & 0 & 0 \end{bmatrix} \quad (11)$$

$$C_{cm} = \begin{bmatrix} 1 & 0 & 0 & 0 & 0 \\ 0 & 0 & 1 & 0 & 0 \end{bmatrix} \quad (12)$$

Above state space systems are then discertized (for the feedback and Kalman filter gains).

3.3 Controllability and Observability

For the state space system where the clutch is open, i.e. the state space system $(A_{o,s}, B_{o,s}, C_{o,s})$, or its discrete form, the controllability matrix is not full rank. This is intuitively obvious since, when the clutch C is open, engine speed state $(x1)$ cannot be controlled by the control input Tm, i.e. motor torque. But, the observability matrix is still full rank. This is because the engine speed state can still be deduced (it is zero, since the engine is disconnected from the drivetrain). Controllability is important during design of the state feedback gains, while observability is important for designing the observer, i.e. Kalman filter. Therefore, when designing the LQR gains, a reduced order model of $(A_{o,s}, B_{o,s}, C_{o,s})$ is used. For designing the observer, the full order system is maintained.

3.4 Kalman filter/Observer Design

As stated above, two of the states (the angles) must be estimated using a Kalman filter, since these are not measurable. Steady state Kalman filter gains are calculated for both modes. Process covariance matrix (Equation 13) and sensor noise covariance matrix (Equation 14) are defined as follows:

$$Sw = \rho \begin{bmatrix} sw_{11} & 0 & 0 & 0 \\ 0 & sw_{22} & 0 & 0 \\ 0 & 0 & sw_{33} & 0 \\ 0 & 0 & 0 & sw_{44} \end{bmatrix} \quad (13)$$

$$Sv = \rho_v \begin{bmatrix} sv_{11} & 0 & 0 \\ 0 & sv_{22} & 0 \\ 0 & 0 & sv_{33} \end{bmatrix} \quad (14)$$

The noise values were based on engineering judgment of prior work. No specific measurements were undertaken for this work. Where ρ and ρ_v tuning scalars. Matlab command 'kalman' is used to obtain Kalman filter gains for the observer for the two modes. State estimation is implemented as a two-step process as shown with equations 15 and 16 below:

Step 1: Prediction:

$$W^-[k] = \left(\alpha.A_{o,s,d} + (1-\alpha).A_{c,s,d}\right) * W^+[k-1] + \left(\alpha.B_{o,s,d} + (1-\alpha).B_{c,s,d}\right).U[k] \quad (15)$$

Where

$W^-[k]$ is the predicted state from the previous state $W^+[k-1]$

$U[k]$ is the input from the current time step

$A_{o,s,d}$ is the state matrix for the open clutch case (suffix 'o') which is scaled and discretized (suffices 's' and 'd' respectively).

$B_{o,s,d}$ is the input matrix for the clutch open case , similarly scaled and discretized.

α is a variable to switch from open clutch case to close clutch case, i.e. when clutch is open, $\alpha = 1$, when clutch is closed, $\alpha = 0$. Decision on the value of α is based on the speed difference between engine and motor speed.

Step 2: Correction:

The state vector prediction in Step 1 of the Kalman filter (equation 15) is now corrected with the most recent measurement (vector 'meas') in equation 16, and the Kalman filter gains L_o , L_c. The vector 'meas', would be a column vector with engine, motor and wheel speed measurement samples.

$$W^+[k] = W^-[k] + (\alpha.L_o + (1-\alpha).L_c).\left(\text{meas} - \left(\alpha.C_{om,s,d} + (1-\alpha)\ .C_{cm,s,d}\right).W^-[k]\right) \quad (16)$$

Where

$W^+[k]$ is the state after correction of $W^-[k]$

$C_{om,s,d}$ is the output matrix (Equation 11) scaled and discretized, for the mode when clutch C is open.
$C_{cm,s,d}$ is the output matrix (Equation 12) scaled and discretized when the clutch C is closed. State vector W can be converted back into the X domain by inverting the scaling operation performed in equation 7.

3.5 Cost Function, Incremental Control for LQR and feedforward control

The objective of the state feedback control is to minimize the jerk, i.e. the rate of change of acceleration, during engine crank and its connection to the drive train. Wheel speed is the fourth state of the system. Matrix $C_{o,s,d}$ in equation 17 represents the scaled, discretized versión of the output matrix Co , when the clutch is open. Change in wheel acceleration over a time step is given by equation 17.

$$\Delta w_4[k] = C_{o,s,d}.\Delta W[k] \quad (17)$$

Where W is the state vector after the scaling.

The jerk can therefore be approximated as

$$J[k] = C_{o,s,d}.\frac{\Delta W[k]}{\Delta T} = C_{o,s,d}.\frac{\Delta W[k]}{\mathrm{Ts}} \quad (18)$$

Let $Q_{o,s,d}$ be the state weighting matrix in the cost function, defined as

$$Q_{o,s,d} = \varrho.\left(\frac{C_{o,s,d}}{Ts}\right)^T\left(\frac{C_{o,s,d}}{Ts}\right) \quad (19)$$

Then, the cost function to minimize jerk can be written in quadratic form as

$$\Im = \frac{1}{2}\sum \Delta W^T Q_{o,s,d}\Delta W + \Delta U^T R \Delta U \quad (20)$$

Where R is a suitable weightage on incremental input (Motor Torque) ΔU. ϱ is a tuning coefficient. Thus, if the LQR state feedback control is implemented in the incremental form [9] (i.e. ΔW and ΔU) instead of W *and* U, then the Jerk can be very easily incorporated in the cost function, and the feedback control law is

$$\Delta U_{fb} = \left(\alpha.K_{o,s,d} + (1-\alpha).K_{c,s,d}\right).\Delta W \quad (21)$$

Where

$K_{o,s,d}$ are the state feedback gains if clutch C is open, $\alpha = 1$

$K_{c,s,d}$ are the state feedback gains if clutch C is closed, $\alpha = 0$.

The LQR gains are calculated using the Matlab function 'dlqr'. Feedforward control has been discussed in literature as an effective method to reject disturbance [10] if it can be modeled with some accuracy. Brake torque (Tb) was considered using feedforward control. The incremental control law (22) is modified to add the feedforward component

$$\Delta U = -\left(\alpha.K_{o,s,d} + (1-\alpha).K_{c,s,d}\right).\Delta W - K_{ff}.\Delta\widehat{Tb} \quad (22)$$

Where

K_{ff} is the feedforward gain, calculated in (23) below.

$$K_{ff} = -\left(C_{o,s,d}.\left(A - B_{o,s,d} * K_{o,s,d}\right)^{-1}.B_{o,s,d}\right)^{-1}.C_{o,s,d}.\left(A - B_{o,s,d}.K_{o,s,d}\right)^{-1}.B_{ow,s,d} \quad (23)$$

The Kalman filter and the feedback, feedforward code was embedded in Simulink as a m-function and cosimulated with the AMESIM plant model.

4. SIMULATION RESULTS

The objective of closed loop control is to eliminate the initial jerk and subsequent sustained oscillations due to actuation of the brake, the throttle, and the clutch . In addition, since not all states are measurable, a Kalman filter was developed to estimate the states associated with the two springs in the system. While elimination of jerk is the objective of the closed loop control, acceleration is a physical measurement that is most used to study measure and quantify disturbances and has been plotted in the results section. Indeed, visual comparison of two acceleration signals can provide a good qualitative idea of the difference in jerk .

4.1 Kalman filter operation

Figure 6 below shows the measured wheel speed (Red) and the predicted wheel speed (blue) using the Kalman filter when the clutch is open and closed. Filtering action of the Kalman filter can be easily seen. To verify the predictive nature of the Kalman filter, the wheel speed measurement (state 4) was removed in figure 7. Figure 7 shows the wheel speed predicted with and without the noisy measurement. The predicted value without the measurement (green) corelates well with the value with measurement (blue).

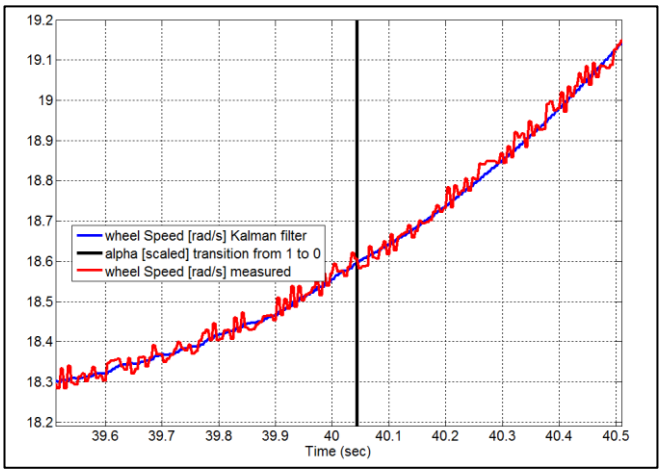

Figure 6. Filtering action of the Kalman filter for wheel speed measurement.

4.2 Rejection of initial jerk during engine crank with closed loop control

Figure 8 below shows the vehicle acceleration response with and without the LQG control (green and red lines, respectively). Comparing the vehicle acceleration with and without the closed loop control (green and red respectively), two observations can be made. The initial jerk (rapid deceleration) between 39 and 39. 5 seconds on the time axis has been elimited. It can be seen that the vehicle acceleration with closed loop control (green) is no longer negative. Thus the driver will not feel a sudden retardation of the vehicle as the engine is cranked. The sudden retardation is caused by the brake (B) acting on the free wheeling ring gear. The negative brake torque is trasferred to the wheels, resulting in the negative acceleration. Inspection of figure 9 suggests that the

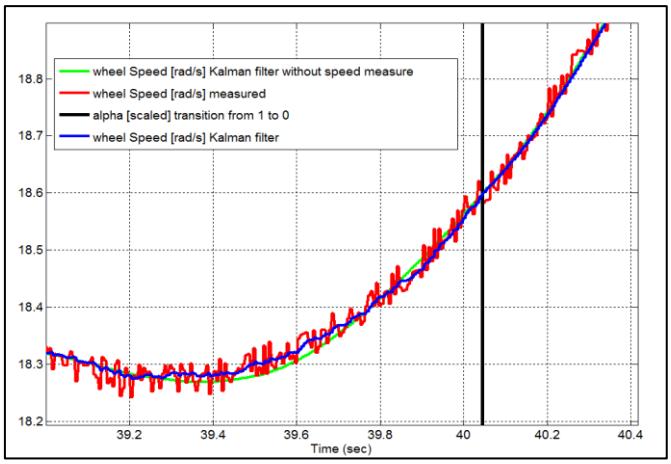

Figure 7. Prediction action of the Kalman filter.

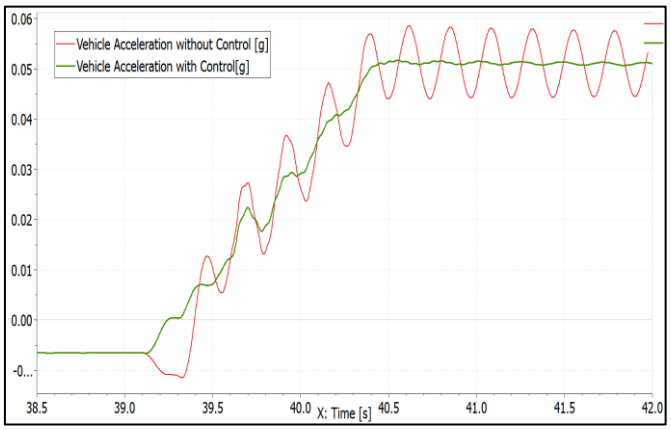

Figure 8. Vehicle acceleration with and without closed loop control

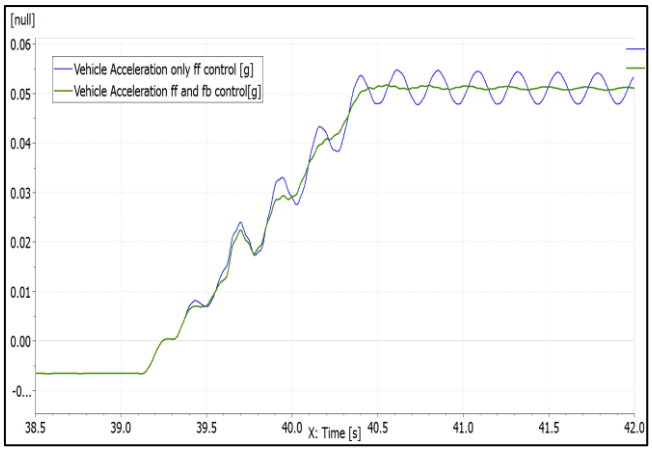

Figure 9. Vehicle acceleration with and without feedback control

cancellation of the initial jerk can be attributed primarily to the feedforward action of the control. Certainly, the motor torque command in figure 10, between 39 and 39.5 seconds, shows significant similarities to the brake torque command (in blue) in figure 4.

4.3 Dampening of the vehicle oscillations (ringing effect)

As discussed in section 2.3, the impulse nature of the brake torque, the throttle command, and the clutch, result in a sustained oscillation along the driveline , as can be seen in the red signal in figure 8. Close loop control eliminates this negative acceleration (green signal in figure 8). Inspection of

figure 9 suggests that the dampening of the oscillations can be attributed to both the feed-forward and the feedback torques. This makes intuitive sense, because elimination of the brake torque impulse by the feedforward torque should reduce the ringing, but not completely eliminate it. The contribution to the ringing effect by the throttle and clutch is eliminated by the feedback control. The sustained oscillations, with the open loop actuation, would have manifested as vibrations felt by the driver and would have been undesirable from a drive quality perspective. Figure 10 shows the motor torque action towards cancelling the sustained oscillations.

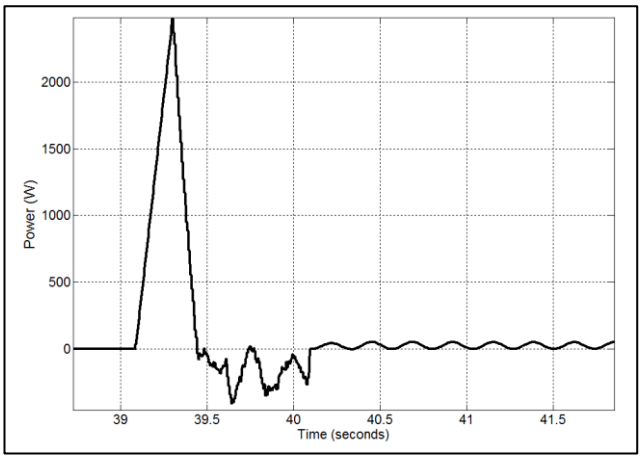

Figure 10. Motor Power for disturbance Rejection

4.4 Motor Utilization to reject disturbances

Figure 10 shows the motor power to reject the disturbance. The peak motor power is about 2.5 kW. The engine crank scenario and the vehicle state during this simulation is one of the harshest from a drive quality perspective. Therefore, it can be concluded that 2.5 kW of motor power should cover all the engine crank disturbances (at other gears and vehicle states). In general, about 2.5 kW of motor power needs to be 'reserved' to be available to reject any disturbance during engine crank, and cannot be used for traction, unless the engine is already operational. This can have an adverse effect on the hybrid vehicle fuel economy. One approach, to ensure that 2.5 kW of motor power is always 'reserved' to cancel engine crank disturbance, is to command /force an engine start as the motor power approaches this 2.5 kW limit. This anticipatory control will eliminate any situation where there is insufficient power reserve, and the engine crank quality suffers.

5. CONCLUSIONS

The simulation results show that the planetary starter can effectively crank an engine for a flying start type of maneuver and Closed loop LQG control has been effective in minimizing the disturbance during the engine cranking and the subsequent oscillations.

In addition, the following comments can be made about this work:

1. The motor torque required to cancel the jerk is heavily influenced by the planetary gear ratio. A lower gear would decrease the brake torque requirement, but would increase the jerk.
2. Certain simplifications are assumed in the model, i.e. no gear lash during transition from negative to positive torque. This would increase the complexity of the model and the associated control. Similarly, motor torque is assumed to be instantaneous, motor electrical time constants, being significantly smaller than the mechanical time constants , have been neglected.
3. Hardware validation of the planetary starter and the control mechanism are needed to validate the simulation results.

REFERENCES

[1] Wu, G., Zhang, X., and Dong, Z (2015). Powertrain Architectures of electrified vehicles: Review, classification, and comparison, *Journal of Franklin Institute*, Volume 352, Issue 2, February 2015, Pages 425-448

[2] Shidore, N., Bucknor, N., and Raghavan M. (2020). Fuel Economy and Drivability Trade-Off for Mild Hybrid Electric Vehicles, *Advances in Industrial Machines and Mechanisms, Select Proceedings of IPROMM 2020,* Pages 709-719.

[3] Christian Jauch, Santosh Tamilarasan, Giorgio Rizzoni et al. (2018). Modeling for drivability and drivability improving control of HEV, *Control Engineering Practice*, Volume 70, January 2108, pages 50-62.

[4] Hao, L., Shidore, N., et al. (2019) .Brushless Fast Starter for Automotive Start/Stop Application", *2019 IEEE Energy Conversion Congress and Exposition (ECCE),* 29 Sep – 3rd Oct 2019, DOI: 10. 1109/ECCE 2019.8912617.

[5] Fulks,G., Roth, G., Fedawa.A. (2012). High Performance Stop-Start System with 14 Volt Belt Alternator Starter. *SAE Int.J.Engines* 5(3):2012, doi:10.4271/2012-01-1041.

[6] Raghavan, M., and Shidore, N. (2020) Hybrid Transmission with gear-based starter and method of starting. *US Patent # US10940748B2.*

[7] Burl, J. (1998) *Linear Optimal Control, H2 and H-infinity methods,* Addison Wesley Publications, California.

[8] Karnopp, D., Margolis, D., Rosenberg, R. (1990) *System Dynamics: A Unified Approach, 2nd edition,* Wiley Interscience Publication, New York.

[9] Peterka, V.(1991) Adaptation of LWG control design to engineering needs*, Advanced Methods in Adaptive Control for Industrial Applications, Lecture notes in control and information Sciences,*Vol 158, Springer , Berlin.

[10] Sievers, L., Andreas H., (1989) Comparison of Two LQG Based Methods for Disturbance Rejection. *Proceedings of the 28th conference on Decision and Control,* Tampa, Florida.

APPENDIX A: AMESIM PLANT MODEL OF THE P2 HYBRID POWERTRAIN